

J.M. LACKNER^{1,✉}
 W. WALDHAUSER¹
 R. EBNER^{1,2}
 R.J. BAKKER³

Chemistry and microstructure of PLD (Ti, Al)C_xN_{1-x} coatings deposited at room temperature

¹ Joanneum Research Forschungsgesellschaft mbH, Laser Centre Leoben,
 Leobner-Strasse 94, 8712 Niklasdorf, Austria

² Materials Center Leoben, Franz-Josef-Strasse 13, 8700 Leoben, Austria

³ Institute of Geological Sciences, University of Leoben, Peter-Tunner-Strasse 5, 8700 Leoben, Austria

Received: 18 September 2003/Accepted: 26 March 2004

Published online: 26 July 2004 • © Springer-Verlag 2004

ABSTRACT The aim of the present work was the improvement of titanium-aluminium nitride (TiAlN) coatings by the solid-solution hardening with carbon atoms leading to titanium-aluminium carbon-nitride (Ti, Al)C_xN_{1-x} coatings with varying carbon (*x*) and nitrogen contents. The request of low deposition temperatures necessary for the coating of heat sensitive materials like tool steels of high hardness and polymers was reached by the application of the room temperature pulsed laser deposition (PLD) technique. A Nd:YAG laser of 1064 nm wavelength operated at two different laser pulse energies was used in the ablation experiments of pure TiAl targets (50 at. % Al) in various C₂H₂-Ar gas mixtures. Different pulse energies of the laser resulted in changes of the ratio of Ti/Al atoms in the grown coatings. Furthermore, the results reveal a strong proportionality of the gas mixture to the C and N content of the coatings. In the coatings deposited at low C₂H₂ gas flows the XRD investigations showed crystalline phases with fcc TiN type lattices, whereas high acetylene flows during deposition resulted in the formation of fully amorphous coatings and carbon precipitation or cluster boundaries found in Raman investigations.

PACS 81.15.Fg; 46.55.+d

1 Introduction

Over the past decade the extension of service life of cutting and forming tools as well as of mechanical components has been successfully achieved by applying thin hard coatings onto their surfaces for reducing the wear and corrosion strains of the substrate materials. TiN, TiCN and TiAlN coatings deposited by different physical vapor deposition (PVD) and chemical vapor deposition (CVD) techniques are now widely accepted in a range of industrial applications where high wear resistance and good adhesion to the substrate are critical [1, 2]. However, there is mounting evidence that the improvement of these coatings by further elements may provide superior performance for some specific applications due to their higher hardness, higher high-temperature strength, higher corrosion resistance, lower friction and lower

wear [3]. Exemplary, some authors reported attractive tribological properties of carbon containing, solid solution hardened TiAlN coatings ((Ti, Al)C_xN_{1-x}) for milling operations at higher cutting speeds and dry working conditions as well as for forging and aluminium diecasting [4–9]. Due to the lack of systematic knowledge of this coating system, the current paper addresses detailed investigations of the role of carbon. Additionally, the deposition was performed at room temperature to comply with the possibility of coating heat sensitive materials.

2 Experimental

High purity Ti-Al targets with a ratio of Ti/Al atoms $R = 1$ (50 at. % Ti, 50 at. % Al) were taken for the ablation experiments using a pulsed Nd:YAG laser with 1064 nm wavelength, 763 and 850 mJ pulse energy, respectively, and 10 ns pulse duration at a repetition rate of 10 Hz. The targets were rotated during the laser irradiation in order to avoid the formation of deep craters. The emitted species were deposited at room temperature in nitrogen containing C₂H₂ atmospheres (ambient pressure ~ 2 – 3 Pa) onto quenched and tempered cold working steel substrates (AISI D2) with a hardness of about 62 HRC and molybdenum sheets with mirror-polished surfaces placed in 100 mm distance to the target surface. The different atmospheres (see Table 1) were chosen in order to produce (Ti, Al)C_xN_{1-x} coatings with varying nitrogen and carbon contents.

The surface quality and the growth structures of the coatings were inspected with a light and a scanning electron microscope (Cambridge Instruments Stereoscan 360). The latter is equipped with a wavelength dispersive analyser (WDS)

Coating/ Sample	Laser pulse energy [mJ]	Gas flow [sccm]	
		C ₂ H ₂	N ₂
C1	763	5	25
C2	763	15	15
C3	850	7.5	22.5
C4	850	10	20
C5	850	30	0

TABLE 1 Deposition parameters (laser pulse energy, C₂H₂ and N₂ gas flow) of the PLD (Ti, Al)C_xN_{1-x} coatings

✉ Fax: +43-3842/812-602-310, E-mail: juergen.lackner@joanneum.at

for chemical analysis. The Raman spectra were obtained by means of a Dilor LABRAM confocal Raman spectrometer operated at a laser wavelength of 633 nm. The laser power of the He-Ne laser was 100 mW, and the spot size was 5 μm . The spectra were taken between 160 to 1600 cm^{-1} with a resolution of 2 cm^{-1} . The phase composition of the (Ti, Al) C_xN_{1-x} coatings were analysed by an X-ray diffractometer (Bruker AXS D8 Discover) using grazing incidence (1.0°) of the primary beam ($\text{Cu } K_\alpha$ radiation).

3 Results and discussion

Quantitative information about the chemical composition of the coatings obtained by WDX investigations is shown in Fig. 1. Two influences of the deposition parameters on the chemical composition can be obtained:

(1) The ratio of Ti/Al atoms R is in all coatings deposited higher than in the target material ($R = 1$) and dependent on the laser pulse energy (Fig. 1a): The higher the laser pulse energy, the higher the Ti contents in the coatings are. This phenomenon can be explained by higher resputtering rates at the substrate surface at higher ion energies, which are present at higher laser pulse energies (laser fluences) [10]. A similar behaviour is reported for Al atoms in TiAlN film deposition [11, 12] decreasing the Al deposition rate and, thus, increasing R . The generally higher content of Ti atoms compared to Al ($R > 1$) in the coatings can only be explained at the homogenous chemical composition of the target ($R = 1$) by considering the whole process of material ablation and deposition. After the ablation the partly ionized metallic vapour is interacting with the reactive gas molecules during the flight phase between the target and the substrate surfaces [13]. Due to the lower atomic mass of Al ($m_{\text{Al}} = 26.98 \text{ g mol}^{-1}$) compared to Ti ($m_{\text{Ti}} = 47.88 \text{ g mol}^{-1}$) the Al atoms in the vapour suffer higher scattering in the collisions with the reactive gas

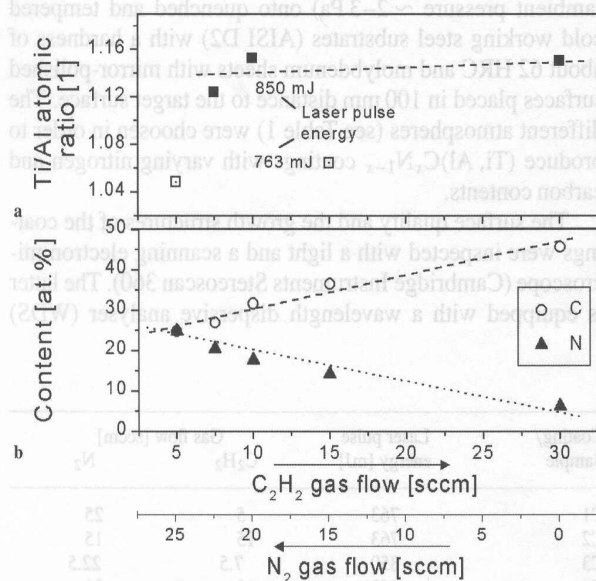


FIGURE 1 Chemical composition of the (Ti, Al) C_xN_{1-x} coatings in dependency on the C_2H_2 and N_2 gas flows applied for deposition: **a** atomic ratio of Ti/Al (pulse energy: \square 763 mJ, \blacksquare 850 mJ), **b** atomic content of carbon and nitrogen

molecules (N_2 , C_2H_2) leading to a lower volume density in the vapour [14]. Thus, the deposition rate of the Ti atoms on the substrate is higher than for Al leading to $R > 1$. Astonishingly, the composition of the gas atmosphere (contents of C_2H_2 and N_2) influence R much less.

(2) In contrast, the C and N contents of the films are strongly influenced by the C_2H_2 and N_2 gas flows during deposition. Thus, it seems to be clear that the collisions of the Ti and Al species (atoms, ions and clusters) with the reactive gas molecules in the vacuum chamber during the flight phase result not only in the scattering of these ablated species, but also in a significant ionization of the process gas necessary for chemical reactions with the ablated species during the flight phase and/or on the substrate surface [13]. An increase of the C_2H_2 or N_2 gas flow results in a nearly linear increase of the C and N content of the coating, respectively (Fig. 1b). The higher reactivity of C_2H_2 molecules in comparison to N_2 molecules can be gathered in the higher C content in the coatings even at low C_2H_2 gas flows. The remaining N_2 content after evacuation of the vacuum recipient is responsible for the low nitrogen content in the coating C5 without N_2 gas flow.

The application of Raman spectroscopy enables the interpretation of the bonding in the (Ti, Al) C_xN_{1-x} coatings. Figure 2 shows the Raman spectra of all coatings deposited and the substrate material. First of all, influences of the substrate on the Raman spectra of the coatings can be excluded. Furthermore, the comparison of the spectra of the (Ti, Al) C_xN_{1-x} coatings with Raman shifts of peak maxima obtained in investigations of TiAlN and TiCN coatings [15, 16] reveals the change from a structure similar to TiAlN to a TiCN structure at higher C_2H_2 flows during deposition leading to higher C contents of the films. In the coatings C1 and C3 with the lowest C contents a broad peak between Raman shifts of 500 and 800 cm^{-1} can be obtained, which is decreased at higher C contents (coating C4) and reduced to a peak around 550 and 650 cm^{-1} for the coatings of the highest C contents (C2, C5). The peak at about 1100 cm^{-1} related to TiCN is present in all coatings, but diminished in

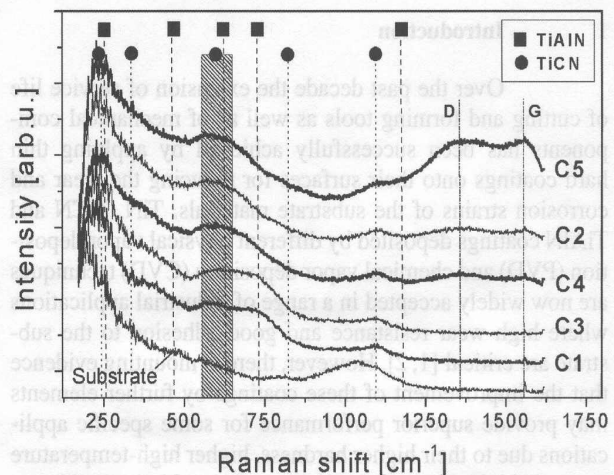


FIGURE 2 Raman spectra of the (Ti, Al) C_xN_{1-x} coatings and the AISI D2 substrate material containing the standard values for TiAlN [15, 16] and TiCN [15] as well as for sp^3 bonded (D) and sp^2 bonded (G) carbon [17]

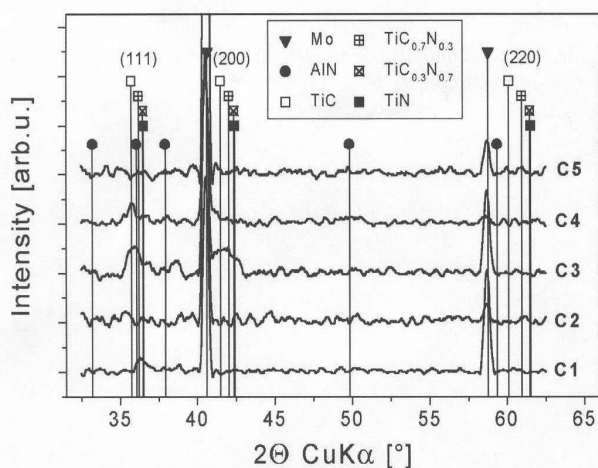


FIGURE 3 Glancing angle (1.0° incidence of the primary beam) XRD spectra of the $(\text{Ti, Al})\text{C}_x\text{N}_{1-x}$ coatings. For comparison the diffraction patterns [20] of TiC, $\text{TiC}_{0.7}\text{N}_{0.3}$, $\text{TiC}_{0.3}\text{N}_{0.7}$, TiN, AlN for the coatings and Mo for the substrate material applied are marked

the coatings with the lower C contents (C1, C3). Furthermore, high C contents in the coatings result in the formation of sp^2 (graphite-like, G) and sp^3 (diamond-like, D) bonded C atoms [17] which are found in the coatings C4, C2, but predominating in coating C5. The D and G peaks found for these coatings reveal pure C precipitations or cluster boundaries in this coating [18, 19].

Grazing incidence XRD analysis of the $(\text{Ti, Al})\text{C}_x\text{N}_{1-x}$ coatings shown in Fig. 3 reveals for coatings of lower C contents (coating C1, C3, C4) crystalline microstructures, whereas the other coatings (C2, C5) seem to be amorphous. The identification of the peaks in the coatings reveals phases with fcc structures similar to TiN or TiC [20]. This structure was expected due to the well known high solubility of Al and C in the fcc NaCl-like TiN lattice [12], which can be attributed to the very similar atomic radii of Ti and Al as well as of C and N atoms. The higher the content of the smaller Al and C atoms (compared to Ti and N atoms, respectively), the higher is the shift to lower diffraction angles. A further influence on the position of the peak maxima of the diffraction pattern is present due to stresses in the coating. Compressive stresses, which are very characteristic for PVD coatings and mainly caused by the growth conditions for room temperature deposited films [21], result in a shift to higher diffraction angles and interfere the shift caused by the chemical composition. Due to these two interfering phenomena – solubility and stresses – a calculation of the lattice stresses in the films from the XRD analyses is not possible [12]. Nevertheless, a qualitative comparison of the crystalline coatings C1, C3 and C4 shows much higher shifts of the (111) peak of the two latter coatings deposited at the higher laser pulse energy of 850 mJ. It is obvious that higher pulse energies lead to a higher degree in ionization of the vapour [10] resulting in higher average energies of the species deposited at the substrate surface [22]. Higher energetic species result in a deeper penetration in the growing film and higher lattice mismatch and, thus, in higher compressive stresses [23]. Besides the higher compressive stresses in the coatings deposited at higher laser pulse energy the (200) fcc peak of TiN and TiC, resp., can be obtained.

The decrease in the intensity of the XRD patterns of the coatings C4 and the lost of XRD patterns of the coatings C2 and C5 with the highest carbon content and, thus, the appearance of amorphous structures can be attributed to the growth of highly carbon containing precipitations or cluster boundaries [16] and the increase of the hydrogen content of the deposition atmosphere which probably increases the hydrogen content in the coatings.

4 Conclusions

$(\text{Ti, Al})\text{C}_x\text{N}_{1-x}$ coatings were deposited by means of the pulsed laser deposition (PLD) technique from a TiAl target with a Nd:YAG laser (wavelength: 1064 nm) in atmospheres of different C_2H_2 and N_2 reactive gas mixtures at room temperature. The variation of the gas mixture strongly influences the carbon and nitrogen content of the coatings. The atomic ratio of Ti/Al was found dependent on the laser pulse energy used in the ablation experiments. At the higher pulse energies used higher Ti contents in the coatings were found. Furthermore, the higher pulse energy leads to higher energies of the ablated species resulting in the higher crystallinity of the coatings. High carbon contents in the coatings prevent, in combination with the hydrogen, the crystallisation of the coatings at the low deposition temperatures (25°C) applied. The appearance of peaks of sp^2 and sp^3 bonded carbon in the Raman spectra indicates the formation of carbon precipitations or cluster boundaries in the coatings.

ACKNOWLEDGEMENTS Financial support of this work by the “Theodor-Körner-Fonds zur Förderung von Wissenschaft und Kunst” of the “Kammer für Arbeiter und Angestellte Wien” is highly acknowledged.

REFERENCES

- 1 M.Y. Al-Jaroudi, H.T.G. Hentzell, S. Gong, A. Bergton: *Thin Solid Films* **195**, 63 (1991)
- 2 H.Z. Wu, T.C. Chou, A. Mishra, D.R. Anderson, J.K. Lampert, C. Gujrathi: *Thin Solid Films* **191**, 55 (1991)
- 3 L.E. Toth: *Refractory Materials*, vol. 7 (Academic Press, New York 1971)
- 4 O. Knotek, F. Löffler, L. Wolkers: *Surf. Coat. Techn.* **68/69**, 176 (1994)
- 5 D. Ileim, R. Hochreiter: *Surf. Coat. Technol.* **98**, 1553 (1998)
- 6 K. Kawata, H. Sugimura, O. Takai: *Thin Solid Films* **390**, 64 (2001)
- 7 O. Knotek, M. Böhmer, T. Leyendecker: *J. Vac. Sci. Techn.* **A4**, 2695 (1986)
- 8 W.-D. Münz: *J. Vac. Sci. Techn.* **A4**, 2717 (1986)
- 9 E. Bernacchi, A. Ferrero, E. Gariboldi, A. Korovkin, G. Pontini: *Metall. Sci. Techn.* **14**, 3 (1996)
- 10 T. Witke, T. Schuelke, J. Berthold, C.F. Meyer, B. Schultrich: *Surf. Coat. Techn.* **116–119**, 609 (1999)
- 11 D.-Y. Wang, Y.-W. Li, C.-L. Chang: *Surf. Coat. Techn.* **114**, 109 (1999)
- 12 S. PalDey, S.C. Deevi: *Mat. Sci. Engin.* **A342**, 58 (2003)
- 13 D.B. Chrisey, G.K. Hubler: *Pulsed Laser Deposition of Thin Films* (John Wiley & Sons, New York 1994)
- 14 R. Wuhler, W.Y. Yeung: *Scripta Mater.* **49**, 199 (2003)
- 15 C.P. Constable, J. Yarwood, W.-D. Münz: *Surf. Coat. Techn.* **116–119**, 155 (1999)
- 16 K.N. Jallad, D. Ben-Amotz: *Wear* **252**, 956 (2002)
- 17 J. Robertson: *Mat. Sci. Engin.* **R37**, 129 (2002)
- 18 Y.L. Su, W.H. Kao: *Wear* **236**, 221 (1999)
- 19 P. Panjan, M. Cekada, D. Kek Merl, M. Macek: *Vacuum* **71**, 261 (2003)
- 20 JCPDF Powder Diffraction File (International Centre for Diffraction 2002)
- 21 B. Rother, J. Vetter: *Plasmabeschichtungsverfahren und Hartstoffschichten* (Deutscher Verlag für Grundstoffindustrie, Leipzig 1992)
- 22 S. Amoroso: *Appl. Surf. Sci.* **138–139**, 292 (1999) 292.
- 23 J.M. Lackner, W. Waldhauser, R. Ebner, B. Major, T. Schöberl: *Thin Solid Films* **181–181C**, 585 (2004)